# Internal conversion in the S_1^1B_[3u] state of pyrene

AUTHOR(S):

Kowaka, Yasuyuki; Nakayama, Naofumi; Ishimoto, Takayoshi; Nagashima, Umpei; Yamanaka, Takaya; Ozawa, Norifumi; Baba, Masaaki

CITATION:

Kowaka, Yasuyuki ...[et al]. Internal conversion in the S_1^1B_[3u] state of pyrene. Chemical Physics 2012, 400: 178-184

ISSUE DATE:

2012-05

URL:

http://hdl.handle.net/2433/156170

# Internal conversion in the $S_1$ $^1B_{3u}$ state of pyrene

Yasuyuki Kowaka[a], Naofumi Nakayama[b], Takayoshi Ishimoto[c], Umpei Nagashima[d,e], Takaya Yamanaka[f], Norifumi Ozawa[a], Masaaki Baba[*,a]

[a] *Division of Chemistry, Graduate School of Science, Kyoto University, Sakyo-ku, Kyoto 606-8502, Japan*
[b] *Conflex Corporation, 2-15-19 Kami-osaki, Shinagawa-ku, Tokyo 141-0021, Japan*
[c] *INAMORI Frontier Research Center, Kyushu University, Motooka 744, Nishi-ku, Fukuoka 819-0395, Japan*
[d] *Research Institute for Nanosystem, National Institute of Advanced Industrial Science and Technology, Umezono 1-1-1, Tsukuba, Ibaraki 305-8561, Japan*
[e] *Core Research for Evolutional Science and Technology, Japan Science and Technology Agency, 4-1-8 Honcho, Kawaguchi 332-0012, Japan*
[f] *Instrument Center, Institute for Molecular Science, Myodaiji, Okazaki 444-8585, Japan*

## Abstract

Fluorescence excitation spectra and fluorescence lifetimes at single vibronic levels in the $S_1$ state have been observed for jet-cooled pyrene. The fluorescence lifetimes at the zero-vibrational levels of the $S_1$ $^1B_{3u}$ states of pyrene-$h_{10}$ and pyrene-$d_{10}$ are 1480 and 1470 ns, respectively, and the relaxation is considered to be dominated by the radiative process. For some vibrational levels, however, the lifetimes are remarkably shorter such as 765 ns at the $22^1$ vibronic level of pyrene-$h_{10}$ ($\nu_{22}$ ($b_{1g}$) ; C-H bending and skeletal deforming mode), indicating that nonradiative transition occurs at a specific vibrational level. In this study, we demonstrate that the main process is internal conversion to the $S_0$ $^1A_g$ state caused by nonadiabatic vibronic interaction via $b_{3u}$ promoting modes.

*Key words:* , pyrene, fluorescence lifetime, internal conversion, ab initio theoretical calculation, molecular structure

*Corresponding author.
E-mail address: baba@kuchem.kyoto-u.ac.jp

## 1. Introduction

Radiationless transitions in large polyatomic molecules are of significant research interest and have been experimentally and theoretically investigated for various isolated molecules [1, 2, 3, 4]. For the $S_1$ $^1B_{2u}$ state of perylene, which is one of the typical polycyclic aromatic hydrocarbons (PAHs), we recently demonstrated that the main radiationless process is internal conversion (IC) to the $S_0$ state and is mode-selective [5, 6]. The fluorescence lifetime has been found to be considerably short for the specific vibrational level of skeletal deforming [7].

For pyrene, It has been demonstrated that the fluorescence lifetime is considerably long at the zero-vibrational level and becomes gradually shorter as the vibrational excess energy increased [8]. However, it is necessary to observe and analyze the fluorescence decay curve more carefully in order to obtain the accurate lifetime value, because the lifetime is long and the decay curve is easily distorted by the experimental setup. Although there has been no report of the accurate measurement of fluorescence quantum yield, radiationless transition processes are assumed to be all very slow and the relaxation in the $S_1$ state is dominated by the radiative transition. The rate of intersystem crossing (ISC) to the triplet state has been demonstrated to be negligible [9]. In the present work, we obtained the accurate fluorescence lifetime at each vibronic level in the $S_1$ state and examined the radiationless transitions.

The fluorescence excitation spectrum for the $S_1 \leftarrow S_0$ transition of pyrene has already been observed in a supersonic jet [8, 9, 10]. Although a normal-mode analysis in the $S_1$ state was carried out, the results were not reliable enough to assign the observed vibronic bands unambiguously. It is therefore necessary to reconsider the results on the basis of ab initio calculation at a sufficiently high level. The $S_1$ state has been identified to be $^1B_{3u}$ [9], in which the absorption band is weak and classified as $^1L_b$ [11]. The molecular structure, and the coordinate (rotational) axes of pyrene are illustrated in Fig. 1. The axis notation is important because the three coordinate axes are equivalent in $D_{2h}$ symmetry. Here we take the $x$ and $y$ axes along the in-plane short and long axes, respectively. The $z$ axis is perpendicular to the molecular plane. In this notation, $^1L_b$ is designated as $^1B_{3u}$, of which the absorption is weak and the radiative lifetime is long. In contrast, $^1L_a$ is designated as $^1B_{2u}$, of which the absorption is strong and the radiative lifetime is short. The strong transition moment is along the $y$ axis. These expressions are identical

to those of linear polyacenes such as naphthalene and anthracene, and this axis notation is favorable to represent the electronic structure of PAHs in general. Mangle and Topp employed another axis notation, of which the expressions are obtained from ours by $x$, $y$, $z$, $B_{1g}$, $B_{2g}$, $B_{3g}$, $B_{1u}$, $B_{2u}$, $B_{3u}$ $\rightarrow$ $y$, $z$, $x$, $B_{3g}$, $B_{1g}$, $B_{2g}$, $B_{3u}$, $B_{1u}$, $B_{2u}$ [8].

The $S_1$ $^1B_{3u}$ state of naphthalene is also assigned to be $^1L_b$. The fluorescence quantum yield is, however, remarkably small ($\sim$ 0.3) and the lifetime is approximately 300 ns [12]. Previously, we demonstrated that the lifetime was markedly shorter for some vibrational levels as a result of efficient IC to the $S_0$ state [13]. These results for pyrene and naphthalene are inconsistent with the general rule that the rate of radiationless transition is proportional to the density of coupling vibrational levels, and that the fluorescence quantum yield becomes smaller as the molecular size becomes larger [2, 4]. It is therefore unusual that no radiationless transition occurs efficiently in a large molecule such as pyrene. This is assumed to be strongly correlated with the fact that the geometrical structure at the zero-vibrational level and the potential energy curve in the $S_1$ state are very similar to those in the $S_0$ state. The vibrational energy may be changed appreciably at the specific normal mode, leading to the shorter fluorescence lifetime.

We performed accurate measurements of the vibrational energies and fluorescence lifetimes for the vibronic bands observed in the fluorescence excitation spectra of jet-cooled pyrene (pyrene-$h_{10}$) and perdeuterated pyrene (pyrene-$d_{10}$). We found that fluorescence lifetime was markedly short at some vibronic levels in the $S_1$ state, of which the vibrational modes were identified on the basis of the results of detailed ab initio calculations. In this article, we present the results of spectral analysis and theoretical calculations and discuss the vibrational structure and IC process at each vibrational level in the $S_1$ $^1B_{3u}$ state of pyrene.

## 2. Experimental

Pyrene-$h_{10}$ (Wako Chemical, 99%) was recrystalized from ethanol and pyrene-$d_{10}$ (Cambridge Isotope Laboratories, 98.4%) was used without further purification. The vapor was mixed with Ar gas (1.5 atm) in a stainless steel container of that was kept at 120 °C. The mixed gas was expanded into a high-vacuum chamber through a pulsed nozzle (an automobile electric fuel injector) to generate a supersonic jet, which was crossed with a pulsed laser beam at right angles. We used a tunable dye laser (Lambda Physik LPD

3002, $\Delta E = 0.1$ cm$^{-1}$, Exalite 398 and 416) pumped by an excimer laser (Coherent Compex Pro 110, 308 nm, 200 mJ). Fluorescence was collected using an ellipsoidal high-reflection mirror to a photomultiplier (Hamamatsu R928), which was set coaxially with the supersonic jet. The transient output was processed by a preamplifier (Stanford research R240, 50Ω, $\Delta t = 10$ ns) and was recorded as a fluorescence decay curve using a storage oscilloscope (LeCroy 9362) .

## 3. Results and Discussion

For the $S_1$ states of pyrene-$h_{10}$ and pyrene-$d_{10}$, we observed the fluorescence excitation spectra in supersonic jets; the results are shown in Fig. 2. Almost all of the prominent vibronic bands are assigned to the transitions from the zero-vibrational level in the $S_0$ state to the $a_g$ and $b_{1g}$ vibrational levels in the $S_1$ state. The vibrational energies of the observed vibronic bands of pyrene-$h_{10}$ and pyrene-$d_{10}$ are listed in Tables 1 and 2, respectively.

Figure 3 depicts the fluorescence decay curves for the $0_0^0$ and $22_0^1$ ($b_{1g}$) ; $0_0^0 + 1111$ cm$^{-1}$ bands of pyrene-$h_{10}$. The linewidth of the exciting laser light is 0.1 cm$^{-1}$, ensuring that a large number of rotational levels are coherently excited. All of the relaxation rates, however, are approximately identical and the fluorescence decay curve is expressed as a single-exponential function,

$$I_f(t) = a\, e^{-\frac{t}{\tau}} \ . \tag{1}$$

The observed curves were well fit by this function and the lifetime ($\tau$) at the zero-vibrational levels of pyrene-$h_{10}$ and pyrene-$d_{10}$ were determined to be 1480 ns and 1470 ns, respectively. The observed values are slightly longer than those reported by Mangle and Topp [8]. This discrepancy is assumed to be due to the fluorescence detection system. The mean speed of molecules in a supersonic jet is over 500 m/s. The excited pyrene molecules translate nearly 1 mm during their lifetime, and some escape from the detection region. In our setup, the photomultiplier is set coaxially with the supersonic jet and the fluorescence is collected using an ellipsoidal reflection mirror, so that the time dependent loss of fluorescence intensity is negligible. It was found that the fluorescence lifetimes of pyrene-$h_{10}$ were appreciably shorter for the specific $b_{1g}$ vibrational levels such as $22^1$, $20^1$, and $16^1$.

For the high-vibrational levels, the decay curve consists of several components with different fluorescence lifetimes. This usually caused by mutual

interaction among the vibrational levels or accidental overlap of vibronic bands. In Fig. 4 are show the decay curves for the $6^1$ ($a_g$) ; $0^0$ + 1397 $cm^{-1}$ level of pyrene-$h_{10}$, and the $5^1$ ($a_g$) ; $0^0$ + 1447 $cm^{-1}$ level of pyrene-$d_{10}$. We approximately expressed the decay curve as a double-exponential function

$$I_f(t) = a_1\, e^{-\frac{t}{\tau_1}} + a_2\, e^{-\frac{t}{\tau_2}}\ . \tag{2}$$

The obtained lifetimes are tabulated in Tables 1 and 2. In order to understand these results, it is essential to analyze the electronic and vibrational structures of the pyrene molecule. We first performed ab initio calculations for the ground $S_0$ $^1A_g$ state to obtain the optimized geometrical structure and rotational constants using the Gaussian 09 program package [14]. The results are listed in Table 3(a) and are compared with the values that were experimentally obtained by ultrahigh-resolution laser spectroscopy [9]. We recently demonstrated that the MP2 method provided approximately the same values of rotational constants in the $S_0$ state as those obtained experimentally for benzene, naphthalene, and anthracene [15, 16]. For pyrene, however, we could not obtain such excellent results using the MP2, HF, and MP4 methods. The DFT(B3LYP)/cc-pVTZ calculation yielded the best result and the differences between the rotational constant values of the experimental and ab initio calculation are 0.08, 0.02, and 0.03% for $A$, $B$, and $C$, respectively. We calculated the vibrational energies for the $a_g$ and $b_{1g}$ normal modes in the $S_0$ state with the optimized structure by this calculational method. We performed least-squares fittings of the observed and calculated vibrational energies, and the best scaling factor was determined to be 0.983. The results are listed in Table 4; they show good agreement with the experimental values.

The transition energies of the $S_1 \leftarrow S_0$ and $S_2 \leftarrow S_0$ $0_0^0$ bands of pyrene-$h_{10}$ have been observed to be 27204 $cm^{-1}$ and 30970 $cm^{-1}$, respectively [10, 9]. It has also been demonstrated by ultrahigh-resolution laser spectroscopy that the $S_1 \leftarrow S_0$ transition moment is in the direction of the in-plane short axis ($x$) and that the $S_1$ state is $^1B_{3u}$. Next, we performed ab initio calculations for the $S_1$ state. We tried several methods to obtain rotational constants with the optimized geometrical structure in the $S_1$ state. The results are presented in Table 3(b). The TD-DFT(cam-B3LYP)/6-31G(d,p) calculation provided values that were very close to the experimentally obtained rotational constants. The calculated excitation energies, however, do not show good agreement with the experimental values. In particular, the excitation

energy of the $^1B_{3u}$ state is delicate because the two excited-state configurations of HOMO $\rightarrow$ LUMO + 1 and HOMO $-$ 1 $\rightarrow$ LUMO are nearly degenerate and are expressed by the same irreducible representation (Fig. 5). These are strongly mixed by the configuration interaction (CI). It is generally difficult to accurately evaluate the effect of CI on the excitation energies. As we could not find an excellent method, we employed the TD-DFT method, which provided very close values of rotational constants to the experimentally obtained ones, to calculate the oscillator strength (absorption intensity) and vibrational energies. The obtained oscillator strengths were $f_{S_1 \leftarrow S_0} = 0.0004$ and $f_{S_2 \leftarrow S_0} = 0.1617$. If the vibrational term is assumed to be unity, the radiative lifetime is given by [17]

$$\tau_r = 1.500 \, \frac{1}{\nu^2 f} \, . \tag{3}$$

We obtained $\tau_r(S_1) = 5100$ ns and $\tau_r(S_2) = 9.7$ ns. Here $\nu$ is the transition wavenumber in units of cm$^{-1}$. These values are consistent with the observed results that the $S_1 \leftarrow S_0$ absorption is weak and that the lifetime of the $S_1$ $^1B_{3u}$ state is fairly long. The calculated vibrational energies of the $a_g$ and $b_{1g}$ modes with the scaling factor of 0.975 are listed in Table 4. The scaling factors are appreciably different for the $S_0$ and $S_1$ states. It indicates that the calculated vibrational energies include some systematic errors arising from using different calculational methods and basis sets. The scaled vibrational energies, however, are in good agreement with expermentally obtained ones for both $S_0$ and $S_1$ states, and this normal mode analysis is considered to be reliable to unambiguously assign the observed vibronic bands.

In the fluorescence excitation spectra, the fundamental vibronic bands of the $a_g$ and $b_{1g}$ modes were observed with comparable intensity to the $0_0^0$ band. The $a_g$ modes are totally symmetric and the vibronic bands are observable for an allowed electronic transition. The transition moment is in the direction of the in-plane short axis ($x$) and the rotational transitions are of $b$-type. The $b_{1g}$ modes are also observable in the fluorescence excitation spectrum, of which the intensities arise from nonadiabatic vibronic interaction with the $S_2$ $^1B_{2u}$ state. The transition moment is, therefore, in the direction of the in-plane long axis ($y$), and the rotational transitions are of $a$-type. In this case, the rotational envelope shows a sharp peak of the $Q$ transitions at the band center. We identified a number of observed vibronic bands by these rotational contours. We also examined the calculated vibrational energies and the resultant assignments are listed in Tables 1 and 2.

The fluorescence lifetimes of vibrational levels are plotted against the vibrational excess energy in Fig. 6. The lifetime becomes gradually shorter as the vibrational excess energy increases and does not change significantly by deuterium substitution. The radiative lifetime is dependent on the electronic transition moment, but is independent of the atomic mass and vibrational energies in the Born−Oppenheimer approximation. The nonradiative lifetime is dominated by non-Born−Oppenheimer or nonadiabatic vibronic interaction, and generally becomes longer by deuterium substitution because the zero-point energy and vibrational overlap with coupling levels are smaller in the deuterated molecule [2, 3, 4]. Consequently, it is considered that the radiationless transition does not occur at the zero-vibrational level in the $S_1$ $^1B_{3u}$ state of pyrene and that is slightly enhanced at the high vibrational levels. The main process is expected to be IC to the $S_0$ $^1A_g$ state. The IC rate at the zero-vibrational level ($v' = 0$) of the $S_1$ state is given by [18]

$$\begin{aligned} W_{IC} \quad \propto \quad & \sum_i \left| \left\langle \phi_{S_0} \left| \frac{\partial}{\partial Q_i} \right| \phi_{S_1} \right\rangle \right|^2 \\ & \times \left| \left\langle \chi_{S_0}^{v''} \left| \frac{\partial}{\partial Q_i} \right| \chi_{S_1}^{v'=0} \right\rangle \right|^2 \\ & \times \delta(E_{S_1}^{v'=0} - E_{S_0}^{v''}) \end{aligned} \tag{4}$$

$$\begin{aligned} \approx \quad & \frac{\sum_i \left| \left\langle \phi_{S_0}(r, Q_0) \left| \left( \frac{\partial U(r,Q)}{\partial Q_i} \right)_{Q_0} \right| \phi_{S_1}(r, Q_0) \right\rangle \right|^2}{\{E_{S_1}(Q_0) - E_{S_0}(Q_0)\}^2} \\ & \times \left| \left\langle \chi_{S_0}^{v''}(Q_i) \left| \frac{\partial}{\partial Q_i} \right| \chi_{S_1}^{v'=0}(Q_i) \right\rangle \right|^2 \\ & \times \left| \prod_{j \neq i} \left\langle \chi_{S_0}^{v''}(Q_j) | \chi_{S_1}^{v'=0}(Q_j) \right\rangle \right|^2 \\ & \times \delta(E_{S_1}^{v'=0} - E_{S_0}^{v''}) \, . \end{aligned} \tag{5}$$

The second factor is the nonadiabatic Franck-Condon overlap of a promoting mode and the third factor is the Franck-Condon overlap of other

modes. For the high vibrational levels in the $S_0$ state, this rate is zero if the potential energy curves along the normal coordinate of a promoting $b_{3u}$ mode are identical for the $S_0$ and $S_1$ states. The equilibrium structures are considered to be nearly identical because the rotational constants are very similar for the $S_0$ and $S_1$ state [9]. The equilibrium C-C bond lengths calculated by the ab initio calculations with geometry optimization are not changed much upon the $S_1 \leftarrow S_0$ excitation, as shown in Table 5. The IC rate is, therefore, expected to be very small at the zero-vibrational level in the $S_1$ $^1B_{3u}$ state of pyrene.

It should be noted that the fluorescence lifetime is remarkably short for some specific vibrational levels. At the $22^1$ level of pyrene-$h_{10}$, the lifetime is 765 ns, which is nearly half that at the zero-vibrational level. The $\nu_{22}$ mode is a vibration of C-H bending (mainly at C(2) and the equivalent positions) and skeletal deforming, so that the $22^1(b_{1g})$ level in the $S_1$ $^1B_{3u}$ state can be coupled with the $b_{2u}$ high vibrational levels in the $S_0$ $^1A_g$ state (direct mechanism). The most probable candidate for the promoting mode is $\nu_{56}$ ($b_{2u}$), of which the nuclear displacement motions are very similar to those of $\nu_{22}$ ($b_{1g}$) with the opposite phase with respect to the long ($y$) axis. These normal coordinates are illustrated in Fig. 7. As for the $22^1$ level, the potential curve in the $S_1$ state is considered to be identical to that in the $S_0$ state because the $\nu_{22}$ vibrational energies are just the same (1111 $cm^{-1}$) for the $S_0$ and $S_1$ states. We assume that the equilibrium structure is slightly different (distortion) [18] along this normal coordinate. The nonadiabatic Franck−Condon overlap is nonvanishing in this case and the IC occurs in the $22^1$ ($b_{1g}$) vibronic level in the $S_1$ $^1B_{3u}$ state, leading to the shorter fluorescence lifetime. The absolute IC rate, is however, still longer than that of naphthalene or anthracene. It is possible to estimate the nonadiabatic Franck−Condon overlap value by numerical calculations of potentials and wavefunctions. However, the high level ab initio calculations are necessary to obtain reliable results for a large molecule such as pyrene. For the IC at the $b_{1g}$ vibronic level, another mechanism is considerable, in which IC takes place by vibronic coupling with the $S_2$ $^1B_{2u}$ state and a $b_{2u}$ promoting mode (indirect mechanism). The contribution is, however, considered to be small because the energy of the $S_2$ state is considerably higher than that of the $22^1$ level in the $S_1$ state. In fact, the observed lifetimes at the $b_{1g}$ levels are not different from those at the $a_g$ levels.

Furthermore, the decay curve is expressed as a double-exponential function at several high vibrational levels. The fast lifetime is approximately 200

ns for all levels, which is attributed to vibronic coupling with the $S_2$ $^1B_{2u}$ state. In particular, the $b_{1g}$ fundamental vibrational levels in the $S_1$ state are strongly coupled and the vibronic bands can be observed as sharp peaks in the fluorescence excitation spectrum. The other weakly coupled levels such as overtones and combination levels yield a broad spectral component. The congested rotational structure due to this vibronic coupling has been observed for the 3068 $cm^{-1}$ level in the $S_1$ $^1B_{3u}$ state of naphthalene [13]. The intensity increases with the vibrational excess energy because the level density and coupling strength become larger. The $S_2$ zero-vibrational level is considered to be mixed with many vibrational levels of the $S_1$ state. The $S_2 \leftarrow S_0$ $0_0^0$ band is broad and is accompanied by satellite bands [10]. This spectral feature is very similar to that of naphthalene [19]. The bandwidth is approximately 10 $cm^{-1}$, indicating that the $S_2 \rightarrow S_1$ IC occurs during 500 ps. In general, the $S_2$ state rapidly transitions to the $S_1$ state and is not fluorescent. This is in accordance with Kasha's rule that the emitting level of a given multiplicity is the lowest level of the multiplicity [20].

## 4. Summary

For the $S_1$ $^1B_{3u}$ state of pyrene-$h_{10}$ and pyrene-$d_{10}$, we observed fluorescence excitation spectra and lifetimes for single vibronic level excitation. The vibrational energies and fluorescence lifetime have been accurately determined for the observed vibronic bands. The lifetimes at the zero-vibrational levels of pyrene-$h_{10}$ and pyrene-$d_{10}$ are 1480 ns and 1470 ns, respectively, and they become gradually shorter as the vibrational excess energy increases. This indicates that radiationless transitions are very slow in the $S_1$ $^1B_{3u}$ state of pyrene. For the $\nu_{22}(b_{1g})$ vibrational level of pyrene-$h_{10}$, however, the fluorescence lifetime is appreciably shorter (765 ns), as a result of IC to the $S_0$ $^1A_g$ state. The $\nu_{22}$ vibration is considered to be the promoting mode of IC in the $S_1$ state. The $\nu_{56}(b_{2u})$ vibration is presumed to be the promoting mode in the $S_0$ state, the nuclear motions of which are very similar to those of $\nu_{22}$ with the opposite phase. For high vibrational levels, the fluorescence decay curve is expressed by a double-exponential function. The fast decay component is originated from many vibrational levels in the $S_1$ state, which are mixed with the $S_2$ state by nonadiabatic vibronic interaction.

## 5. Acknowledgements

This research was supported by a Grant-in-Aid for the Global COE Program, "International Center for Integrated Research and Advanced Education in Materials Science", from the Ministry of Education, Culture, Sports, Science and Technology of Japan. The authors would like to thank to N. Takada, S. Sugito, H. Miyashita, N. Takamatsu, M. Aoyama, M. Kondo, T. Yano, N. Mizutani, and M. Suzui (Equipment Development Center, Institute for Molecular Science, Japan) for creating an ellipsoidal mirror for high-efficiency fluorescence collection.

## References

[1] P. Avouris, W. M. Gelbart, M. A. El-Sayed, Chem. Rev. 77 (1977) 793.

[2] M. Bixon, J. Jortner, J. Chem. Phys. 48 (1968) 715.

[3] K. F. Freed, Acc. Chem. Res. 1 (1978) 74.

[4] S. H. Lin, J. Chem. Phys. 44 (1966) 3759.

[5] Y. Kowaka, Y. Suganuma, N. Ashizawa, N. Nakayama, H. Goto, T. Ishimoto, U. Nagashima, M. Baba, J. Mol. Spectrosc. 260 (2010) 72.

[6] Y. Suganuma, Y. Kowaka, N. Ashizawa, N. Nakayama, T. Ishimoto, U. Nagashima, T. Yamanaka, T. Ueda, N. Nishi, M. Baba, Mol. Phys. 109 (2011) 1831.

[7] A. J. Kaziska, S. A. Wittmeyer, A. L. Motyka, M. R. Topp, Chem. Phys. Lett. 154 (1989) 199.

[8] E. A. Mangle, M. R. Topp, J. Phys. Chem. 90 (1986) 802.

[9] M. Baba, M. Saitoh, Y. Kowaka, K. Taguma, K. Yoshida, Y. Semba, S. Kasahara, Y. Ohshima, T. Yamanaka, Y.-C. Hsu, S. H. Lin, J. Chem. Phys. 131 (2009) 224318.

[10] N. Ohta, H. Baba, G. Marconi, Chem. Phys. Lett. 133 (1987) 222.

[11] J. R. Platt, J. Chem. Phys. 17 (1949) 484.

[12] F. M. Behlen, S. A. Rice, J. Chem. Phys. 75 (1981) 5672.

[13] K. Yoshida, Y. Semba, S. Kasahara, T. Yamanaka, M. Baba, J. Chem. Phys. 130 (2009) 194304.

[14] M. J. Frisch, G. W. Trucks, H. B. Schlegel, G. E. Scuseria, M. A. Robb, J. R. Cheeseman, G. Scalmani, V. Barone, B. Mennucci, A. F. Izmaylov, J. Bloino, G. Zheng, J. L. Sonnenberg, M. Hada, M. Ehara, K. Toyota, R. Fukuda, J. Hasegawa, M. Ishida, T. Nakajima, Y. Honda, O. Kitao, H. Nakai, T. Vreven, J. A. Montgomery, Jr., J. E. Peralta, F. Ogliaro, M. Bearpark, J. J. Heyd, E. Brothers, K. N. Kudin, V. N. Staroverov, R. Kobayashi, J. Normand, K. Raghavachari, A. Rendell, J. C. Burant,

S. S. Iyengar, J. Tomasi, M. Cossi, N. Rega, J. M. Millam, M. Klene, J. E. Knox, J. B. Cross, V. Bakken, C. Adamo, J. Jaramillo, R. Gomperts, R. E. Stratmann, O. Yazyev, A. J. Austin, R. Cammi, C. Pomelli, J. W. Ochterski, R. L. Martin, K. Morokuma, V. G. Zakrzewski, G. A. Voth, P. Salvador, J. J. Dannenberg, S. Dapprich, A. D. Daniels, O. Farkas, J. B. Foresman, J. V. Ortiz, J. Cioslowski, D. J. Fox, Gaussian09, Revision A.02, Gaussian Inc., Wallingford, CT, 2009.

[15] M. Baba, Y. Kowaka, U. Nagashima, T. Ishimoto, H. Goto, N. Nakayama, J. Chem. Phys. 135 (2011) 054305.

[16] M. Baba, M. Saitoh, K. Taguma, K. Shinohara, K. Yoshida, Y. Semba, S. Kasahara, N. Nakayama, H. Goto, T. Ishimoto, U. Nagashima, J. Chem. Phys. 101 (2009) 134315.

[17] R. A. Becker, Theory and Interpretation of Fluorescence and Phosphorescence, John Wiley & Sons, New York, 1969.

[18] W. Siebrand, J. Chem. Phys. 46 (1967) 440.

[19] S. M. Beck, D. E. Powers, J. B. Hopkins, R. E. Smalley, J. Chem. Phys. 73 (1980) 2019.

[20] M. Kasha, Disc. Faraday Soc. 9 (1950) 14.

Table 1. Vibrational energies ($cm^{-1}$), lifetimes (ns) and assignments of the bands observed in the fluorescence excitation spectrum of the $S_1$ $^1B_{3u} \leftarrow S_0$ $^1A_g$ transition of pyrene-$h_{10}$.

| Vibrational energy | Lifetimes $\tau_1$ | $\tau_2$ | $(a_2)$ [a] | Assignment |
|---|---|---|---|---|
| 0 | | 1480 | | $0_0^0$ (27204 $cm^{-1}$) |
| 393 | | 1190 | | $13_0^1$ ($a_g$) |
| 443 | | 1190 | | |
| 449 | | 1250 | | $25_0^1$ ($b_{1g}$) |
| 453 | | 1250 | | |
| 494 | | 1210 | | $24_0^1$ ($b_{1g}$) |
| 551 | | 1190 | | |
| 572 | | 1080 | | $12_0^1$ ($a_g$) |
| 673 | | 957 | | |
| 709 | | 973 | | |
| 724 | | 1060 | | |
| 730 | | 1200 | | $23_0^1$ ($b_{1g}$) |
| 782 | | 1170 | | $11_0^1$ ($a_g$) |
| 1023 | 238 | 905 | (1.9) | $10_0^1$ ($a_g$) |
| 1111 | | 765 | | $22_0^1$ ($b_{1g}$) |
| 1144 | | 1120 | | $9_0^1$ ($a_g$) |
| 1250 | 147 | 837 | (3.4) | $20_0^1$ ($b_{1g}$) |
| 1282 | 160 | 853 | (1.9) | |
| 1298 | 220 | 867 | (0.84) | |
| 1357 | 75 | 974 | (10.1) | $19_0^1$ ($b_{1g}$) |
| 1397 | 147 | 1090 | (1.3) | $6_0^1$ ($a_g$) |
| 1575 | 250 | 794 | (2.2) | $16_0^1$ ($b_{1g}$) |
| 1681 | | 840 | | $4_0^1$ ($a_g$) |
| 1699 | | 840 | | |
| 1841 | | 783 | | |
| 1902 | 204 | 804 | (3.7) | |
| 1942 | 178 | 664 | (3.2) | |

[a] Relative values assuming $a_1 = 1$.

Table 2. Vibrational energies ($cm^{-1}$), lifetimes (ns) and assignments of the bands observed in the fluorescence excitation spectrum of the $S_1$ $^1B_{3u} \leftarrow S_0$ $^1A_g$ transition of pyrene-$d_{10}$.

| Vibrational energy | Lifetimes $\tau_1$ | $\tau_2$ | $(a_2)$ [a] | Assignment |
|---|---|---|---|---|
| 0 | | 1470 | | $0_0^0$ (27283 $cm^{-1}$) |
| 384 | | 1270 | | $13_0^1$ ($a_g$) |
| 431 | | 1300 | | $25_0^1$ ($b_{1g}$) |
| 460 | | 1220 | | $24_0^1$ ($b_{1g}$) |
| 544 | | 1240 | | $12_0^1$ ($a_g$) |
| 607 | | 1280 | | |
| 645 | | 1140 | | |
| 682 | | 1180 | | $23_0^1$ ($b_{1g}$) |
| 698 | | 1220 | | |
| 735 | | 1180 | | $11_0^1$ ($a_g$) |
| 743 | | 1230 | | |
| 770 | 205 | 1170 | (4.5) | |
| 832 | 188 | 1130 | (4.5) | $10_0^1$ ($a_g$) |
| 856 | | 1200 | | $9_0^1$ ($a_g$) |
| 927 | | 1170 | | |
| 932 | | 1160 | | $21_0^1$ ($b_{1g}$) |
| 1008 | | 1090 | | |
| 1225 | | 972 | | $19_0^1$ ($b_{1g}$) |
| 1231 | | 989 | | $7_0^1$ ($a_g$) |
| 1245 | | 951 | | |
| 1289 | | 1050 | | |
| 1323 | | 1080 | | |
| 1348 | | 970 | | |
| 1382 | 201 | 1060 | (2.1) | |
| 1390 | | 929 | | $17_0^1$ ($b_{1g}$) |
| 1403 | | 978 | | $18_0^1$ ($b_{1g}$) |
| 1430 | | 905 | | $6_0^1$ ($a_g$) |
| 1447 | 214 | 871 | (9.2) | $5_0^1$ ($a_g$) |
| 1557 | | 882 | | $16_0^1$ ($b_{1g}$) |
| 1822 | | 777 | | |

[a] Relative values assuming $a_1 = 1$.

Table 3. Experimental and calculated rotational constants ($cm^{-1}$) in the $S_0$ $^1A_g$ state of pyrene-$h_{10}$.

| | Rotational constants | | |
|---|---|---|---|
| | $A$ | $B$ | $C$ |
| (a) $S_0$ $^1A_g$ | | | |
| exp [a] | 0.0339147 | 0.0186550 | 0.0120406 |
| DFT(B3LYP)/cc-pVTZ | 0.0339412 | 0.0186518 | 0.0120370 |
| MP2/cc-pVTZ | 0.0338789 | 0.0186461 | 0.0120269 |
| HF/6-31G(d,p) | 0.0340442 | 0.0187661 | 0.0120976 |
| MP4(SDQ)/6-31G(d,p) | 0.0336811 | 0.0185206 | 0.0119497 |
| (b) $S_1$ $^1B_{3u}$ | | | |
| exp [a] | 0.0336223 | 0.0184864 | 0.0119329 |
| TD-DFT(cam-B3LYP)/6-31G(d,p) | 0.0336785 | 0.0185127 | 0.0119752 |
| SAC-CI/6-31G(d,p) | 0.0335954 | 0.0185335 | 0.0119442 |
| CASSCF/6-31G(d,p) | 0.0338710 | 0.0184180 | 0.0119305 |
| RCIS/6-31G(d,p) | 0.0341973 | 0.0184529 | 0.0119855 |

[a] Ref.9.

Table 4. Calculated and observed $a_g$ and $b_{1g}$ vibrational energies ($cm^{-1}$) in the $S_0$ $^1A_g$ and $S_1$ $^1B_{3u}$ states of pyrene-$h_{10}$ and pyrene-$d_{10}$.

| | | | Pyrene-$h_{10}$ | | | | Pyrene-$d_{10}$ | | | |
|---|---|---|---|---|---|---|---|---|---|---|
| | | | $S_0$ $^1A_g$ | | $S_1$ $^1B_{3u}$ | | $S_0$ $^1A_g$ | | $S_1$ $^1B_{3u}$ | |
| | Number | Vibration type | Calc.[a] | (Obs.) [b] | Calc.[c] | (Obs.)[d] | Calc.[a] | | Calc.[c] | (Obs.)[d] |
| $a_g$ | 1 | C-H stretch | 3143 | | 3105 | | 2357 | | 2299 | |
| | 2 | C-H stretch | 3134 | | 3089 | | 2347 | | 2288 | |
| | 3 | C-H stretch | 3118 | | 3077 | | 2326 | | 2268 | |
| | 4 | C-C stretch | 1646 | (1624) | 1663 | (1681) | 1689 | | 1646 | |
| | 5 | C-C stretch + C-H bend | 1572 | | 1530 | | 1509 | | 1472 | (1447) |
| | 6 | C-C stretch | 1406 | (1410) | 1442 | (1397) | 1465 | | 1429 | (1430) |
| | 7 | ring deform | 1333 | (1326) | 1326 | | 1305 | | 1273 | (1231) |
| | 8 | ring deform + C-H bend | 1245 | (1238) | 1257 | (1250) | 1181 | | 1152 | |
| | 9 | C-H bend | 1152 | (1140) | 1141 | (1144) | 853 | | 860 | ( 856) |
| | 10 | ring deform + C-H bend | 1076 | (1072) | 1046 | (1023) | 882 | | 832 | ( 832) |
| | 11 | ring deform | 804 | ( 805) | 779 | ( 782) | 753 | | 734 | ( 735) |
| | 12 | ring breathing | 587 | ( 593) | 570 | ( 572) | 559 | | 545 | ( 549) |
| | 13 | ring deform | 406 | ( 402) | 393 | ( 393) | 395 | | 385 | ( 384) |
| $b_{1g}$ | 14 | C-H stretch | 3126 | | 3082 | | 2334 | | 2276 | |
| | 15 | C-H stretch | 3115 | | 3071 | | 2322 | | 2264 | |
| | 16 | C-C stretch | 1608 | (1571) | 1563 | (1575) | 1584 | | 1545 | (1557) |
| | 17 | C-C stretch + C-H bend | 1513 | (1513) | 1492 | | 1460 | | 1424 | (1403) |
| | 18 | C-C stretch | 1415 | | 1425 | | 1448 | | 1412 | (1390) |
| | 19 | C-H bend + ring deform | 1381 | (1372) | 1408 | (1357) | 1259 | | 1228 | (1225) |
| | 20 | C-H bend + ring deform | 1247 | (1238) | 1242 | (1250) | 1064 | | 1038 | |
| | 21 | C-H bend | 1183 | (1212) | 1167 | | 959 | | 935 | ( 932) |
| | 22 | C-H bend + ring deform | 1112 | (1111) | 1101 | (1111) | 855 | | 834 | |
| | 23 | ring deform | 739 | ( 735) | 729 | ( 730) | 701 | | 683 | ( 683) |
| | 24 | ring deform | 501 | ( 500) | 499 | ( 494) | 472 | | 461 | ( 459) |
| | 25 | ring deform | 456 | ( 451) | 449 | ( 449) | 443 | | 432 | ( 432) |

[a] Results of DFT(B3LYP)/cc-pVTZ are scaled by 0.983.
[b] Determined using the dispersed fluorescence spectrum [Ref.9].
[c] Results of TD-DFT(cam-B3LYP)/6-31G(d,p) are scaled by 0.975.
[d] Determined using the fluorescence excitation spectrum in the present work.

Table 5. Calculated C-C bond lengths (Å) of pyrene in the $S_0$ $^1A_g$ and $S_1$ $^1B_{3u}$ states.

| | $S_0$ $^1A_g$ [a] | $S_1$ $^1B_{3u}$ [b] |
|---|---|---|
| $R_{\text{C-C}}$( 1- 2) | 1.3882 | 1.4002 |
| $R_{\text{C-C}}$( 2-11) | 1.3988 | 1.4020 |
| $R_{\text{C-C}}$(11- 3) | 1.4331 | 1.4216 |
| $R_{\text{C-C}}$( 3- 4) | 1.3552 | 1.3715 |
| $R_{\text{C-C}}$(11-15) | 1.4230 | 1.4487 |
| $R_{\text{C-C}}$(15-16) | 1.4217 | 1.4217 |

[a] DFT(B3LYP)/cc-pVTZ calculation.
[b] TD-DFT(cam-B3LYP)/6-31G(d,p) calculation.

## Figure Captions

**Fig. 1** Molecular structure and coordinate (rotational) axes of pyrene.

**Fig. 2** Fluorescence excitation spectra of jet-cooled (a) pyrene-$h_{10}$ and (b) pyrene-$d_{10}$.

**Fig. 3** Fluorescence decay curves for excitations of (a) $0_0^0$ and (b) $22_0^1$ ($0_0^0$ + 1111 cm$^{-1}$) bands of pyrene-$h_{10}$.

**Fig. 4** Fluorescence decay curves for excitations of (a) $6_0^1$ band of pyrene-$h_{10}$ and (b) $5_0^1$ band of pyrene-$d_{10}$.

**Fig. 5** $\pi$ molecular orbitals and the electronic configurations for the $S_1$ $^1B_{3u}$ and $S_2$ $^1B_{2u}$ states.

**Fig. 6** Fluorescence lifetimes for vibronic levels in the $S_1$ $^1B_{3u}$ states of (a) pyrene-$h_{10}$ and (b) pyrene-$d_{10}$. Circles, squares, and triangles indicate the $a_g$, $b_{1g}$, and unassigned levels, respectively.

**Fig. 7** Normal coordinates of (a) $\nu_{22}$ ($b_{1g}$) and (b) $\nu_{56}$ ($b_{2u}$). The observed $\nu_{22}$ and calculated $\nu_{56}$ vibrational energies are shown below.

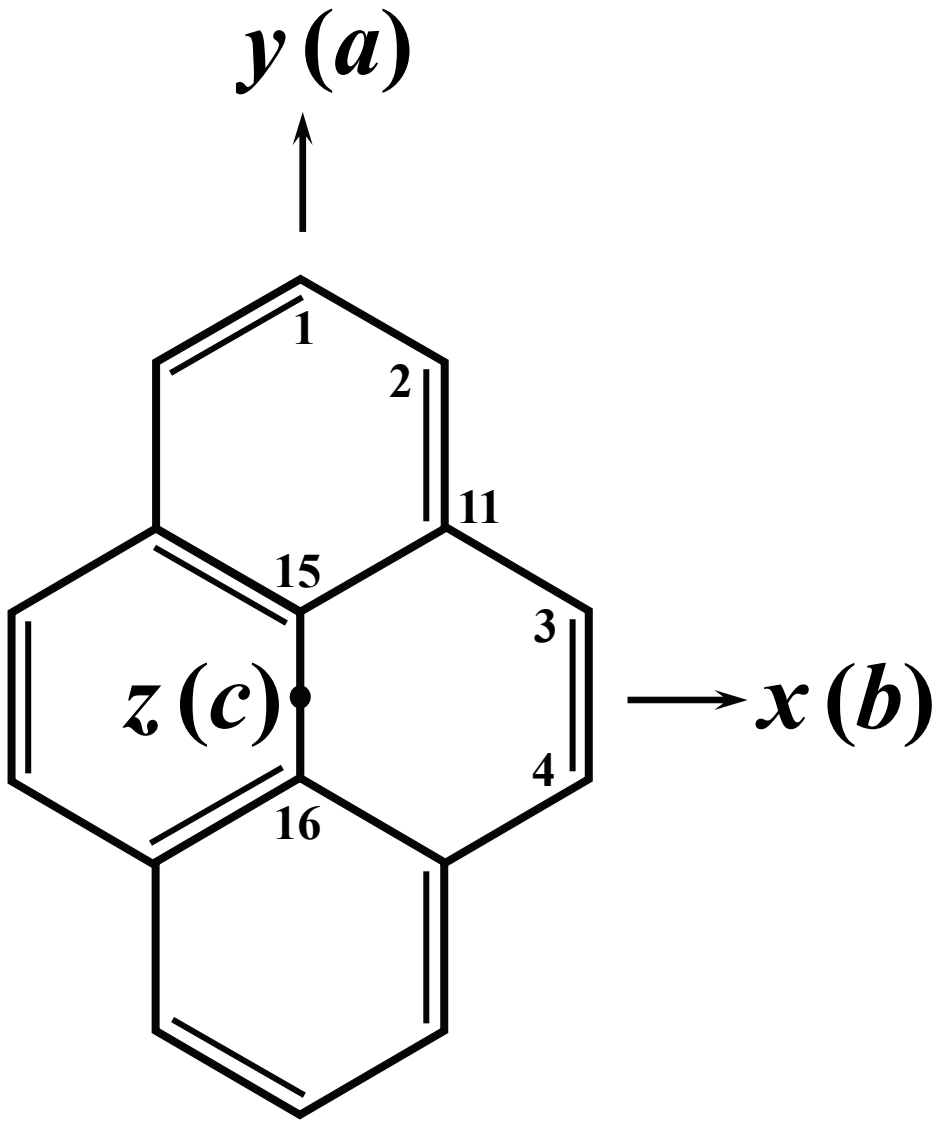


**Fig. 1.** Y. Kowaka *et al.*

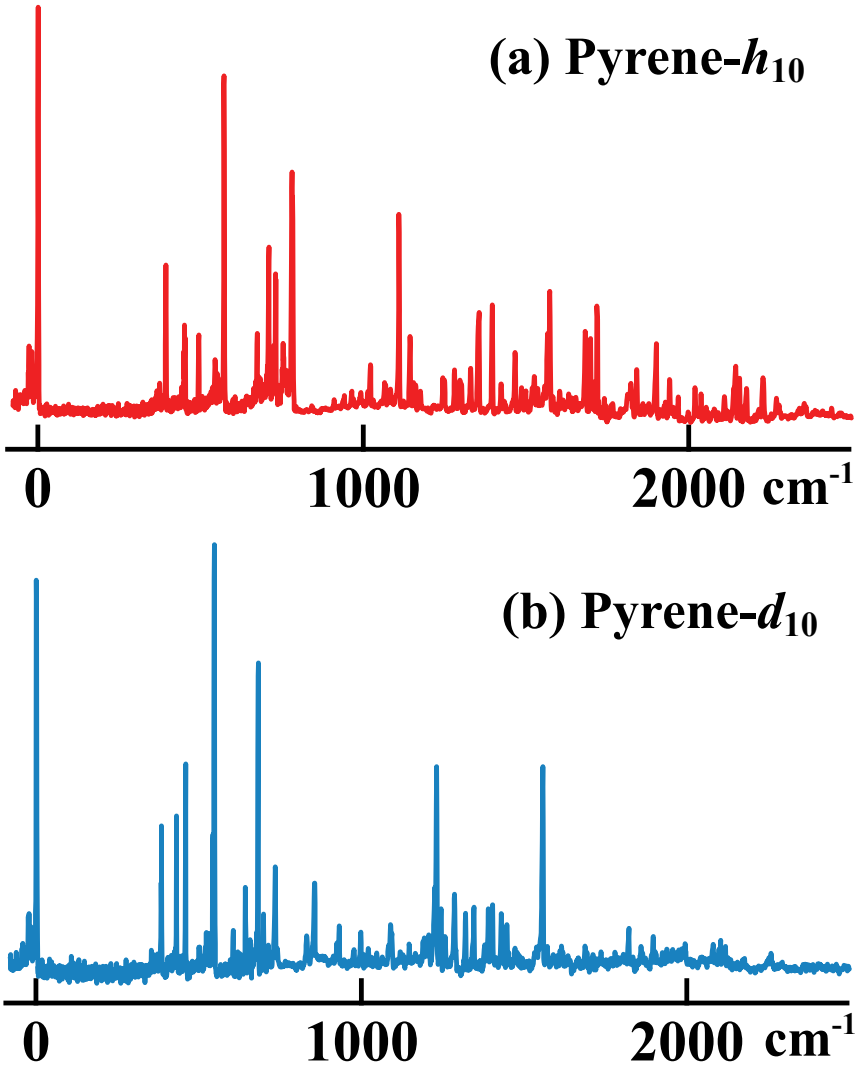


**Fig. 2. Y. Kowaka *et al.***

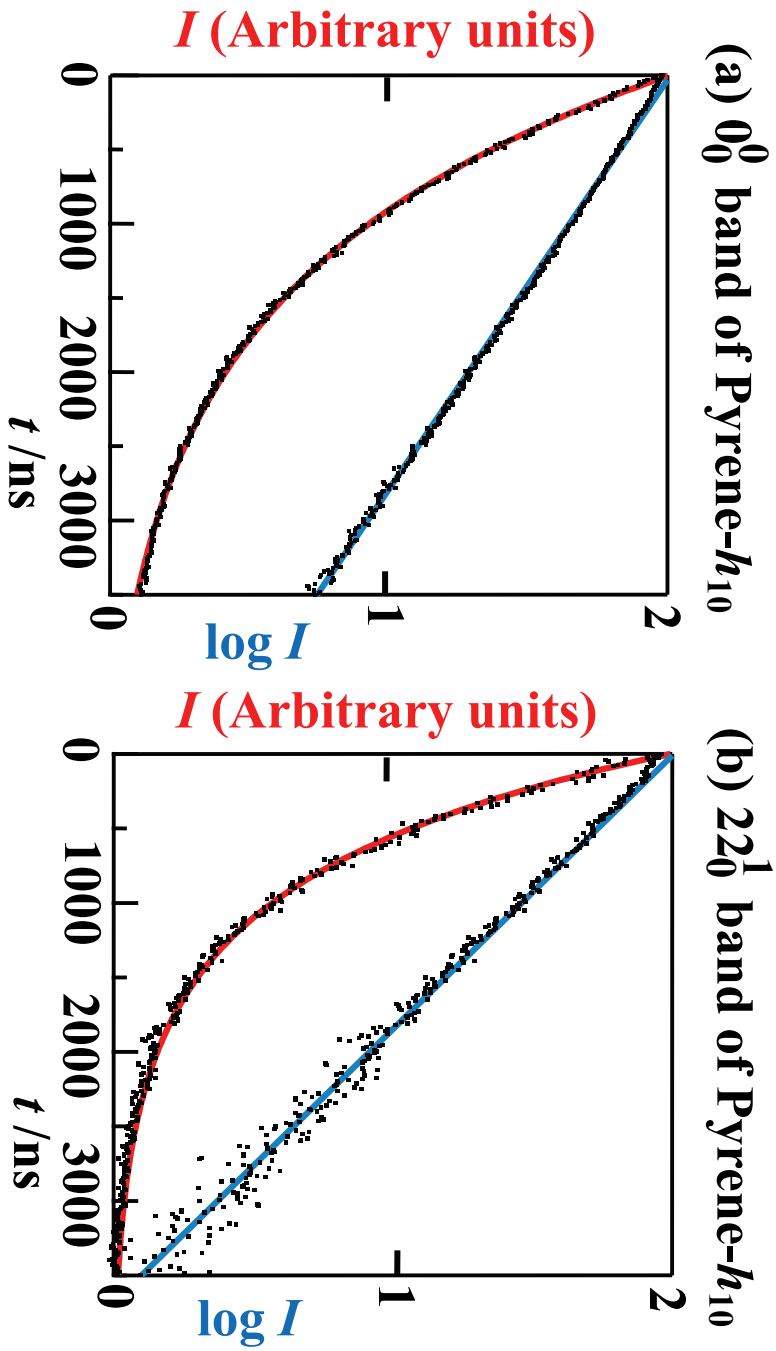


**Fig. 3.** **Y. Kowaka *et al.***

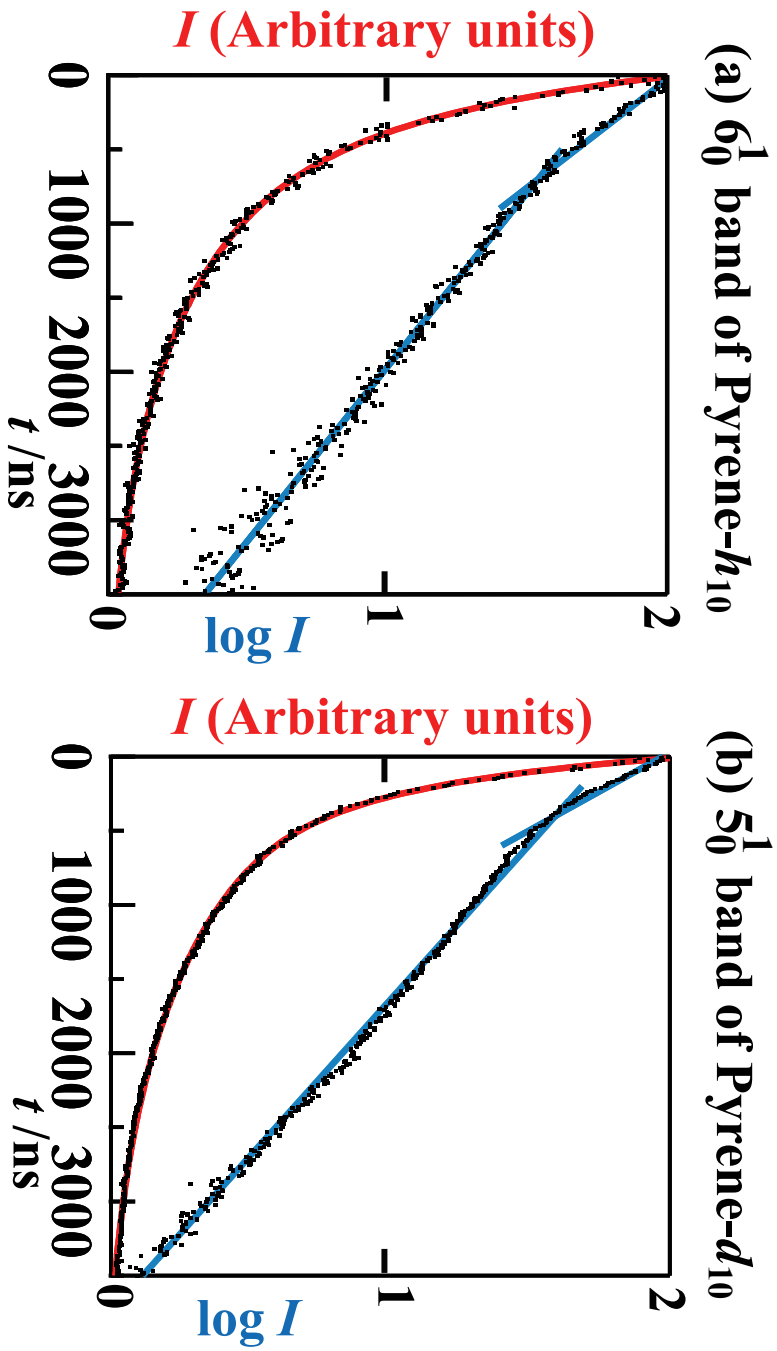


**Fig. 4.** **Y. Kowaka *et al.***

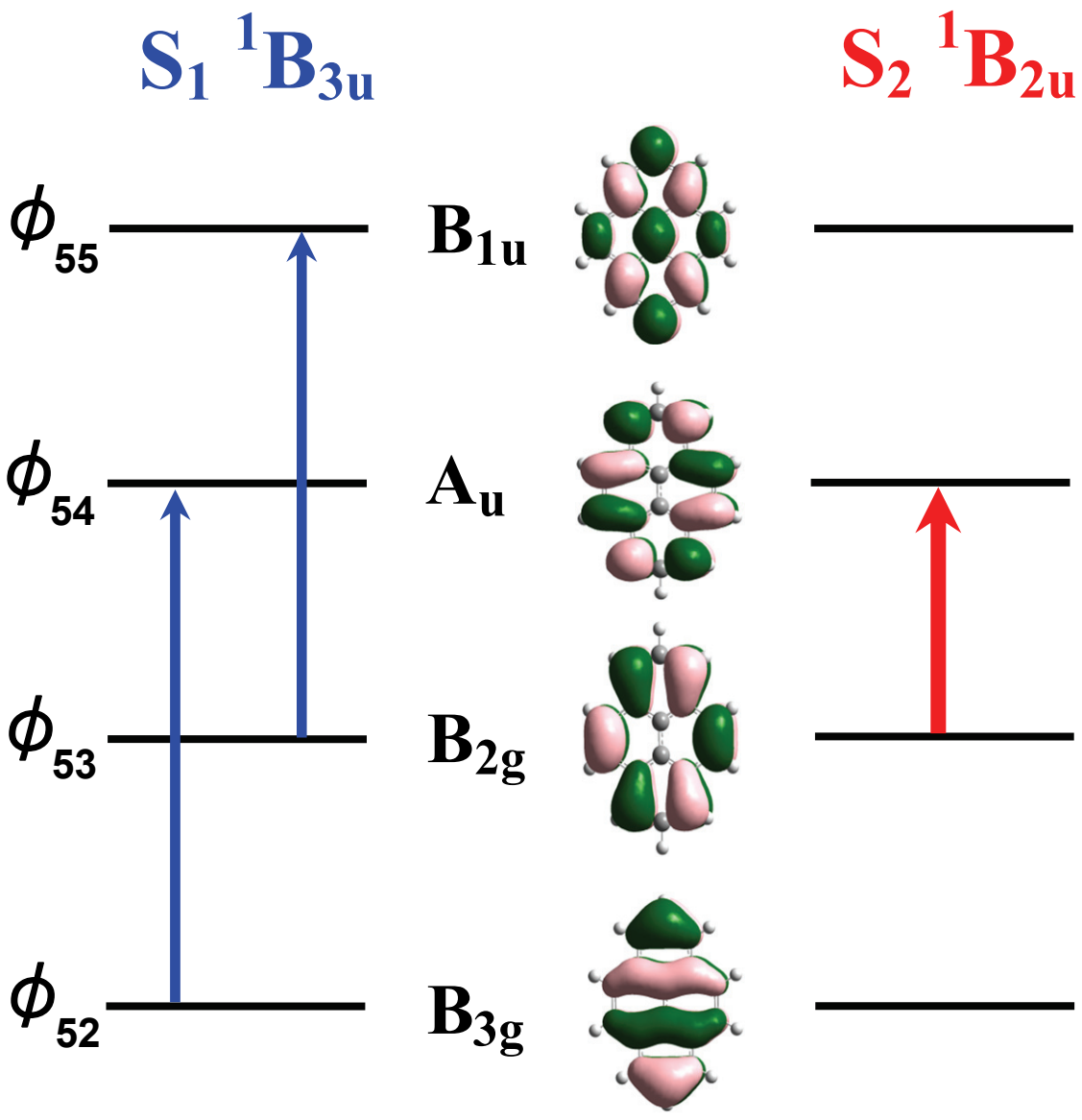


**Fig. 5.** Y. Kowaka *et al.*

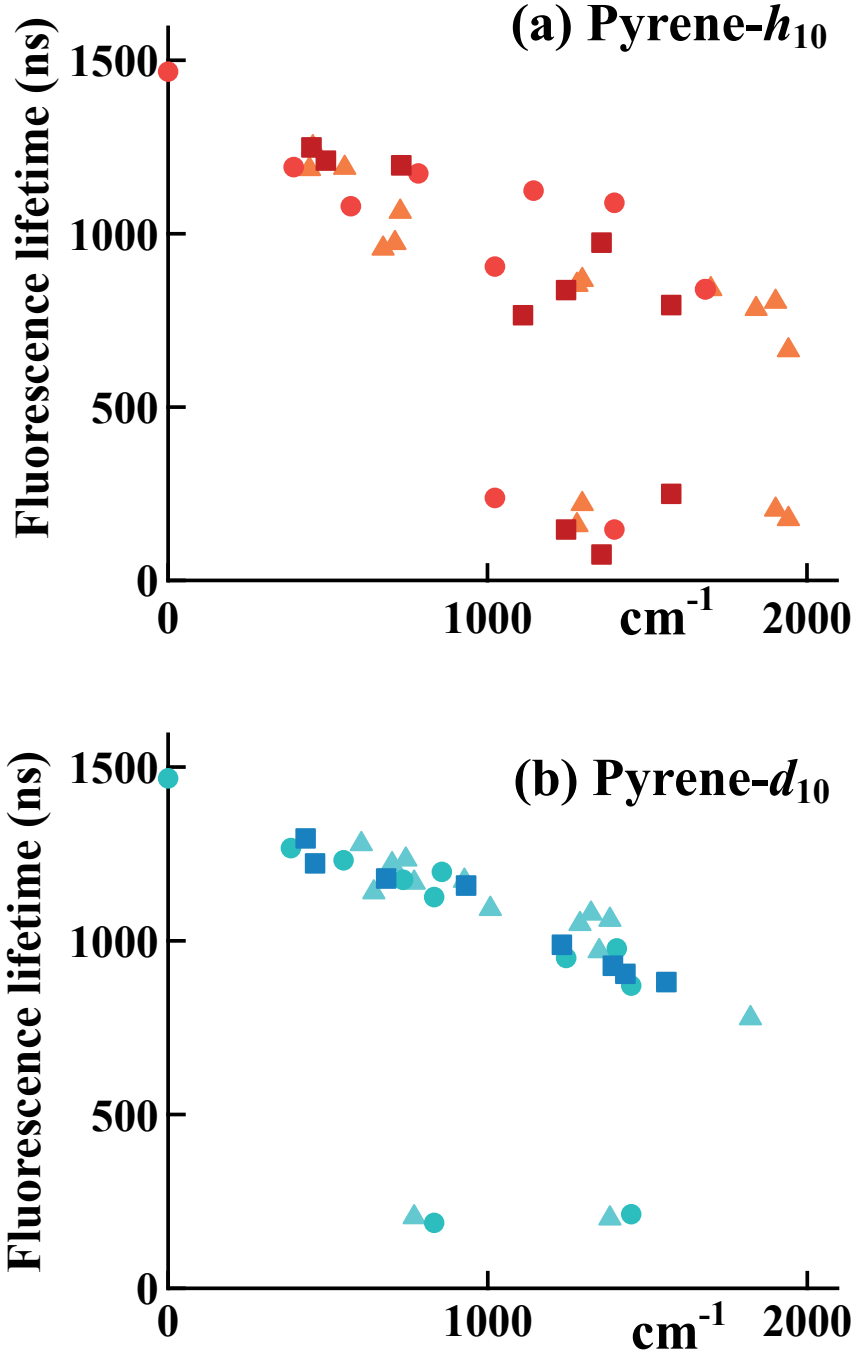


**Fig. 6.** Y. Kowaka *et al.*

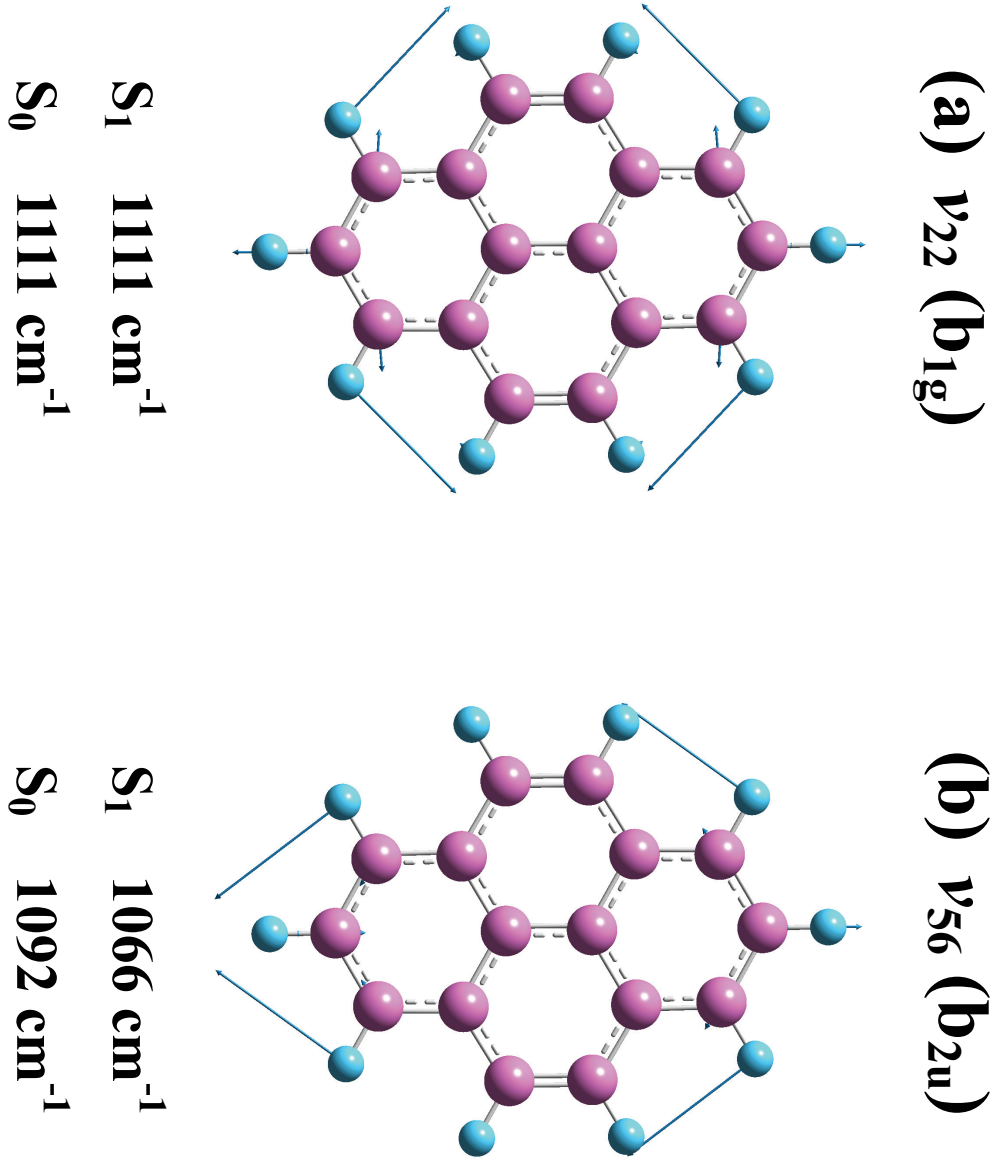


**Fig. 7.** **Y. Kowaka *et al.***